DARK ENERGY SURVEY

Chiara Coviello
Supervisor: James Annis

University of Pisa
Fermilab Summer School 2022

29 August 2022

DARK ENERGY

Through Friedmann equations, which are Einstein equation ($G_{\mu\nu} = 8\pi G T_{\mu\nu}$) in FRWL metric ($ds^2 = -dt^2 + a^2(t)[dr^2/(1-kr^2) + r^2(d\theta^2 + sin^2\theta d\phi^2)]$), we find:

$$\Omega_K + \Omega_\Lambda + \Omega_M + \Omega_R = 1 \quad (1)$$

$$q = \frac{\Omega}{2}(1 + 3\omega) \quad (2)$$

where $\Omega_K = -\frac{k}{a^2 H^2}$, $\Omega_i = \frac{\rho_i}{\rho_{crit}}$, $\rho_{crit} = \frac{3H^2}{8\pi G}$, $p = \omega\rho$, $q = -\frac{\ddot{a}}{aH^2}$, $H = \frac{\dot{a}}{a}$

Notice that $q < 0$ if $\omega < -1/3$

High redshift ($1 + z = \frac{a(t_0)}{a(t_s)}$) measurements can say if the Universe expansion is accelerated or not (Hubble law at 2^{nd} order: $H_0 d_L = z + \frac{1}{2}(1 - q_0)z^2$)

Observations say that we are in an accelerated Universe!

So what is going on?

THE NATURE OF DARK ENERGY

- Beyond Standard Model: new kind of matter *(scalar fields with vacuum energy* $\neq 0$ *and with* $\omega < -1/3$*. For example* $\mathcal{L} = \frac{1}{2}\partial_\mu Q \partial^\mu Q + V(Q)$*, if* $\dot{Q} << V(Q)$ *then* $\omega \sim -1$*)*

- Modified General Relativity:
  - $S = \frac{1}{16\pi G}\int d^4x\sqrt{-g}F(\phi)R$
  - gravitons mass $\neq 0$

ΛCDM COSMOLOGICAL MODEL

In ΛCDM cosmological model $\omega = -1$ and $\rho_\Lambda = \frac{\Lambda}{8\pi G} \sim const$, *where* Λ *is the cosmological term*. The model parameters are: $\Omega_\Lambda \simeq 0.7$ $\Omega_M \simeq 0.3$ $\Omega_B \simeq 0.05$ $\Omega_R \simeq \Omega_K \simeq 0$; the difference between Ω_M and Ω_B is attributed to dark matter

There are different possible explanation to the "dark matter problem", e.g.: 1)PARTICLES, of which the classic ones are WIMP; 2) MACHOS, almost planetary compact objects; 3) MOND, $F = ma$ *for* $a > a_0$ *and* $F = ma^2/a_0$ *for* $a < a_0$ *with* $a_0 \simeq 10^{-10} ms^{-1}$*; 4)WAVE-LIKE, axions are the classical candidates.*

THE DARK ENERGY SURVEY

DES is a six-year survey that mapped 5000 deg^2 of the southern sky in five broadband filters using 570 megapixel Dark Energy Camera. The optically-selected catalog is built using redMaPPer algorithm

GOAL: testing the ΛCDM model and studying the nature of dark energy

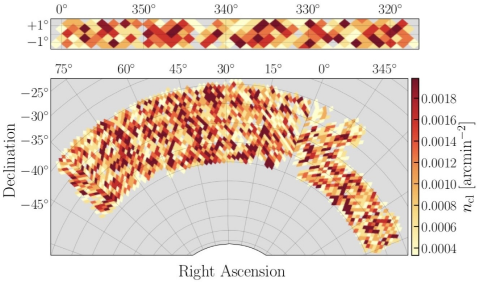

FIG. 1. The DES Y1 redMaPPer cluster density over the two non-contiguous regions of the Y1 footprint: the Stripe 82 region (116 deg^2; *upper* panel) and the SPT region (1321 deg^2; *lower* panel).

GRAVITATIONAL LENSING

Galaxy Cluster: SMACS 0723

Image credit: NASA, ESA, CSA, and STScI, James Webb Space Telescope, 2022 (infrared)

Galaxy Cluster: Abell 370

Image Credit: NASA, ESA, Hubble, 2019 (visible)

DES Y1 DATA

1. THE NUMBER OF GALAXY CLUSTERS in bins of richness and redshift
2. THE AVERAGE MASS OF THE GALAXY CLUSTERS in said bins

TABLE I. Number of galaxy clusters in the DES Y1 redMaPPer catalog for each richness and redshift bin. Each entry takes the form $N(N) \pm \Delta N$ stat $\pm \Delta N$ sys. The numbers between parenthesis correspond to the number counts corrected for the miscentering bias factors (see section III A). The first error bar corresponds to the statistical uncertainty in the number of galaxy clusters in that bin, and is the sum of a Poisson and a sample variance term. The systematic error is due to miscentering errors in the redMaPPer catalog (see text for details).

λ	$z \in [0.2, 0.35)$	$z \in [0.35, 0.5)$	$z \in [0.5, 0.65)$
$[20, 30)$	762 (785.1) $\pm$ 54.9 $\pm$ 8.2	1549 (1596.0) $\pm$ 68.2 $\pm$ 16.6	1612 (1660.9) $\pm$ 67.4 $\pm$ 17.3
$[30, 45)$	376 (388.3) $\pm$ 32.1 $\pm$ 4.5	672 (694.0) $\pm$ 38.2 $\pm$ 8.0	687 (709.5) $\pm$ 36.9 $\pm$ 8.1
$[45, 60)$	123 (127.2) $\pm$ 15.2 $\pm$ 1.6	187 (193.4) $\pm$ 17.8 $\pm$ 2.4	205 (212.0) $\pm$ 17.1 $\pm$ 2.7
$[60, \infty)$	91 (93.9) $\pm$ 14.0 $\pm$ 1.3	148 (151.7) $\pm$ 15.7 $\pm$ 2.2	92 (94.9) $\pm$ 14.2 $\pm$ 1.4

TABLE II. Mean mass estimates for DES Y1 redMaPPer galaxy clusters in each redshift bin. The reported quantities are $\log_{10}(\mathrm{M})$ where masses are defined using a 200-mean overdensity criterion ($M_{200\mathrm{m}}$). The masses are measured in $h^{-1}\mathrm{M}_\odot$ and include the selection effect correction discussed in Appendix D. The first error bar refers to the statistical error in the recovered mass, while the second error bar corresponds to the systematic uncertainty.

λ	$z \in [0.2, 0.35)$	$z \in [0.35, 0.5)$	$z \in [0.5, 0.65)$
$[20, 30)$	14.036 $\pm$ 0.032 $\pm$ 0.045	14.007 $\pm$ 0.033 $\pm$ 0.056	13.929 $\pm$ 0.048 $\pm$ 0.072
$[30, 45)$	14.323 $\pm$ 0.031 $\pm$ 0.051	14.291 $\pm$ 0.031 $\pm$ 0.061	14.301 $\pm$ 0.041 $\pm$ 0.086
$[45, 60)$	14.454 $\pm$ 0.044 $\pm$ 0.050	14.488 $\pm$ 0.044 $\pm$ 0.065	14.493 $\pm$ 0.056 $\pm$ 0.068
$[60, \infty)$	14.758 $\pm$ 0.038 $\pm$ 0.052	14.744 $\pm$ 0.038 $\pm$ 0.052	14.724 $\pm$ 0.061 $\pm$ 0.069

The binning scheme is driven by the need to achieve high signal-to-noise measurements of the weak-lensing profile of the galaxy cluster

SYSTEMATIC UNCERTAINTIES IN CLUSTER MASS CALIBRATION

Source of systematic	SV Amplitude uncertainty	Y1 Amplitude Uncertainty
Shear measurement	4%	1.7%
Photometric redshifts	3%	2.6%
Modeling systematics	2%	0.73%
Cluster triaxiality	2%	2.0%
Line-of-sight projections	2%	2.0%
Membership dilution + miscentering	$\leqslant 1\%$	0.78%
Total Systematics	6.1%	4.3%
Total Statistical	9.4%	2.4%
Total	11.2%	5.0%

-Shear multiplicative bias: an over- or under-estimation of gravitational shear;

-Redshift systematic uncertainties;

-Miscentering: the fraction of correctly centered redMaPPer clusters is $f_{cen} = 0.75 \pm 0.08$;

-Modeling systematics: inaccuracies in the halo-mass correlation function model;

-Selection effects: correlation between cluster richness and lensing signal at a fixed mass;

-Projection effects: changes in cluster lensing and λ due to matter and galaxies projected along the line of sight;

-Triaxiality: dark matter haloes have triaxial shapes.

SYSTEMATIC UNCERTAINTIES IN CLUSTER COUNTS

The covariance matrix of cluster counts is due to Poisson noise, sample variance and cluster miscentering

THEORETICAL MODEL

$$\langle N\rangle = \int_0^\infty dz^{true} \int_{z_{min}}^{z_{max}} dz^{ob} \int_{\lambda_{min}}^{\lambda_{max}} d\lambda^{ob} \langle n|\lambda^{ob}, z^{true}\rangle \frac{dV}{dz^{true}} P(z^{ob}|z^{true}) \qquad (3)$$

$$\langle M\rangle = \frac{1}{\langle N\rangle} \int_0^\infty dz^{true} \int_{z_{min}}^{z_{max}} dz^{ob} \int_{\lambda_{min}}^{\lambda_{max}} d\lambda^{ob} \langle nM|\lambda^{ob}, z^{true}\rangle \frac{dV}{dz^{true}} P(z^{ob}|z^{true}) \qquad (4)$$

$$\langle \lambda^{sat}|M,z\rangle = \left(\frac{M - M_{min}}{M_1 - M_{min}}\right)^{\alpha} \left(\frac{1+z}{1+z_*}\right)^{\epsilon} \quad with \quad \lambda^{true} = \lambda^{cen} + \lambda^{sat} \qquad (5)$$

$\langle n|\lambda^{ob}, z^{true}\rangle$: *comoving space density of clusters;* $\langle nM|\lambda^{ob}, z^{true}\rangle$: *mass weighted comoving density;* $\frac{dV}{dz^{true}}$: *survey volume per unity redshift;* λ^{cen}: *number of central galaxies (*λ^{cen}*=1 for* $M \geq M_{min}$ *and =0 otherwise);* λ^{sat}: *number of satellite galaxies (random variable);* M_1: *characteristic mass at which a halo of mass* M *has on average one satellite galaxy;* λ^{ob} *is a noisy measurement of* λ^{true}*.*

RESULTS

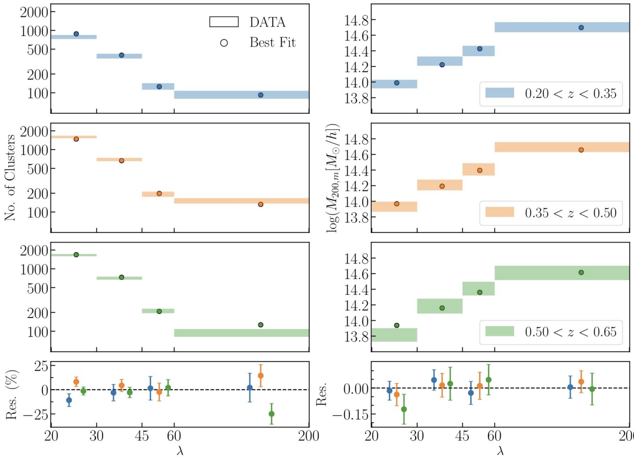

FIG. 2. Observed (*shaded areas*) and best-fit model (*dots*) for the cluster number counts (*left*) and mean cluster masses (*right*) as a function of richness for each of our three redshift bins. The y extent of the data boxes is given by the square root of the diagonal terms of the covariance matrix. The bottom panel shows the residual between the data and our best-fit model. All points have been slightly displaced along the richness axis to avoid overcrowding.

COSMOLOGICAL CONSTRAINTS

TABLE III. Model parameters and parameter constraints from the joint analysis of redMaPPer DES Y1 cluster abundance and weak-lensing mass estimates. In the third column we report our model priors: a range indicates a top-hat prior, while $\mathcal{N}(\mu, \sigma)$ stands for a Gaussian prior with mean μ and variance σ^2. The fourth column lists the modes of the 1-d marginalized posterior along with the 1-σ errors. Parameters without a quoted value are those for which the marginalized posterior distribution is the same as their prior.

Parameter	Description	Prior	Posterior
Ω_m	Mean matter density	$[0.0, 1.0]$	$0.179^{+0.031}_{-0.038}$
$\ln(10^{10}A_s)$	Amplitude of the primordial curvature perturbations	$[-3.0, 7.0]$	4.21 ± 0.51
σ_8	Amplitude of the matter power spectrum	–	$0.85^{+0.04}_{-0.06}$
$S_8 = \sigma_8(\Omega_m/0.3)^{0.5}$	Cluster normalization condition	–	$0.65^{+0.04}_{-0.04}$
$\log M_{min}[\mathrm{M}_\odot/h]$	Minimum halo mass to form a central galaxy	$(10.0, 14.0)$	11.13 ± 0.18
$\log M_1[\mathrm{M}_\odot/h]$	Characteristic halo mass to acquire one satellite galaxy	$\log(M_1/M_{\min}) \in [\log(10), \log(30)]$	12.37 ± 0.11
α	Power-law index of the richness–mass relation	$[0.4, 1.2]$	0.748 ± 0.045
ϵ	Power-law index of the redshift evolution of the richness–mass relation	$[-5.0, 5.0]$	-0.07 ± 0.28
σ_{intr}	Intrinsic scatter of the richness–mass relation	$[0.1, 0.5]$	< 0.325
s	Slope correction to the halo mass function	$\mathcal{N}(0.047, 0.021)$	–
q	Amplitude correction to the halo mass function	$\mathcal{N}(1.027, 0.035)$	–
h	Hubble rate	$\mathcal{N}(0.7, 0.1)$	0.744 ± 0.075
$\Omega_b h^2$	Baryon density	$\mathcal{N}(0.02208, 0.00052)$	–
$\Omega_\nu h^2$	Energy density in massive neutrinos	$[0.0006, 0.01]$	–
n_s	Spectral index	$[0.87, 1.07]$	–

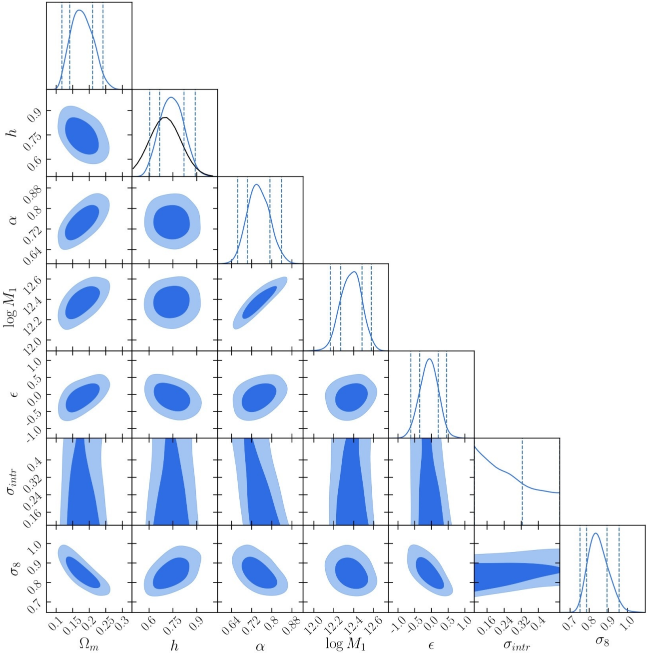

h
α
$\log M_1$
ϵ
σ_{intr}
σ_8
Ω_m
h
α
$\log M_1$
ϵ
σ_{intr}
σ_8

COMPARISON WITH OTHER CONSTRAINTS FROM THE LITERATURE

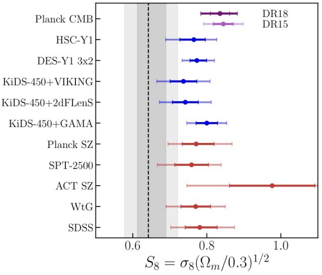

FIG. 5. Comparison of the 68% (*dark*) and 95% (*light*) confidence level constraints on S_8 derived from our baseline model (*shaded gray* area) with other constraints from the literature: *red* error bars for cluster abundance analyses, *blue* error bars for weak lensing and galaxy clustering analyses and *purple* for the CMB constraint. From the bottom to the top: SDSS from [19]; WtG from [7]; ACT SZ from [68] (BBN+H0+ACTcl(dyn) in the paper); SPT-2500 from [9]; Planck SZ from [69] (CCCP+H_0+BBN in the paper); KiDS-450+GAMA from [70]; KiDS-450+2dFLens from [71]; KiDS-450+VIKING from [72]; DES-Y1 3x2 from [20]; HSC-Y1 from [11]; *Planck* CMB from [73] (DR15) and [2] (DR18). Note that all the constraints but those from SDSS, DES-Y1 3x2, HSC-Y1 and Planck CMB have been derived fixing the total neutrino mass either to zero or to 0.06 eV.

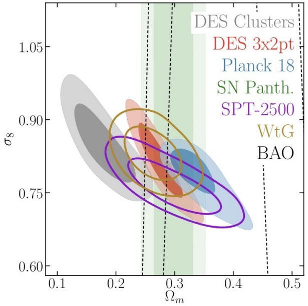

FIG. 6. Comparison of the 68% and 95% confidence contours in the σ_8-Ω_m plane derived from DES Y1 cluster counts and weak-lensing mass calibration (*gray* contours) with other constraints from the literature: BAO from the combination of data from Six Degree Field Galaxy Survey [6dF 62], the SDSS DR 7 Main galaxy sample [63], and the Baryon Oscillation Spectroscopic Survey [BOSS 64] (*black dashed* lines); Supernovae Pantheon [65] (*green* contours); DES-Y1 3x2 from [20] (*red* contours); *Planck* CMB from [2] (*blue* contours); SPT-2500 from [9] (*violet* contours); WtG from [7] (*gold* contours).

SELECTION EFFECT BIAS

It induces correlation between lensing signal and cluster richness at fixed mass

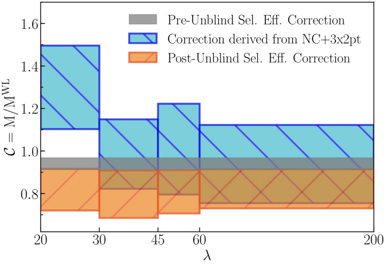

FIG. 12. *Cyan bars*: Mean correction required to reconcile the weak-lensing mass estimates from [15] – without the triaxiality and projection effects corrections – with the mean masses predicted by the combination of Y1 cluster counts and 3x2pt cosmology. Also over-plotted the projection and triaxiality effects correction estimated analytically in [15] and adopted pre-unblinding (*gray band*), and the selection effect correction adopted post-unblinding (*orange bars*). The y extent of the bars represent the 68% confidence interval; the *cyan* bars are estimated as the ratio of the masses predicted by randomly sampling the NC+3x2pt chain, and the "raw" weak-lensing masses randomly drawn from their posterior distribution.

OUR WORK

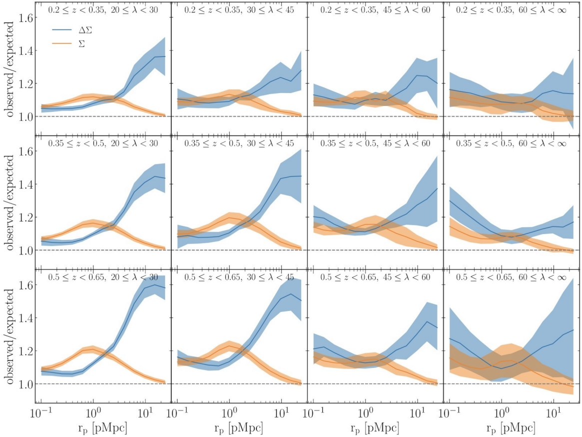

❶ MODEL

- Observed/expected Σ: $\Pi(R) = \begin{cases} \Pi_0 (R/R_0) & \textit{for } R \leq R_0 \\ \Pi_0 + c\, \ln(R/R_0) & \textit{for } R > R_0 \end{cases}$

  Π_0 and R_0 are defined for each richness bin, while c is shared across all richness bins.
- Observed/expected $\Delta\Sigma$: parabola

❷ TIMING

Compare the time that cluster toolkit and ccl need in order to compute $\Delta\Sigma$ and see which one is faster

CCL:

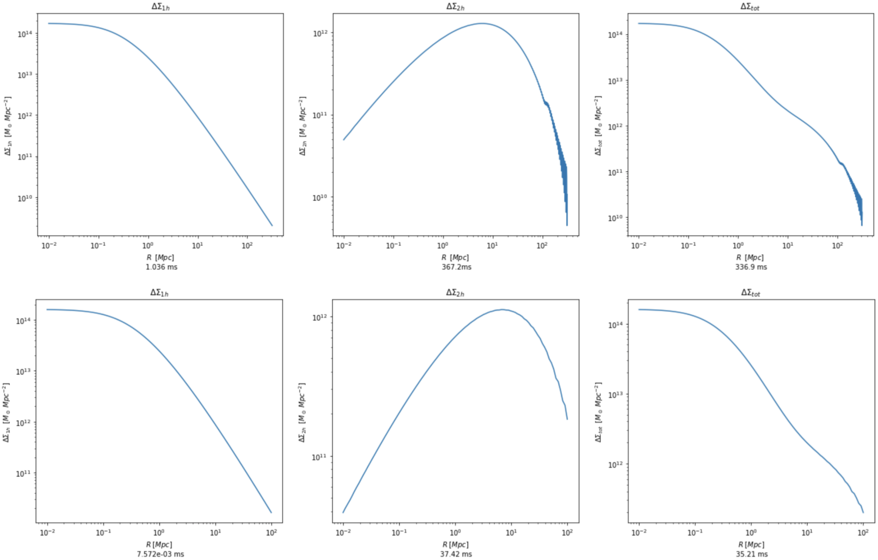

cluster toolkit:

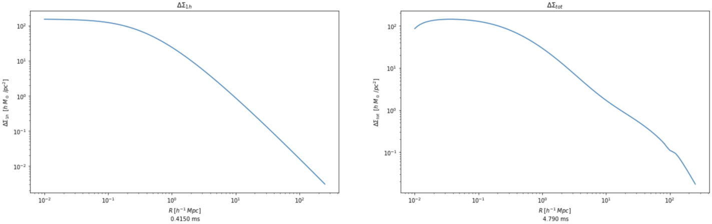

③ PIPELINE

Write a new pipeline to include selection effects in the chosen toolkit

④ COSMOLOGY

See what are the cosmology constraints this new analysis leads to

⑤ THEORY

Try to find theoretical explanations to the results

⑥ FUTURE

If it turns out that selection bias is not the solution, the next steps will be: think about other possible systematics/effects and continue considering the possibility that there could be some cluster physics which is still not known

BIBLIOGRAPHY

- Dark Energy Survey Year 1 Results: Cosmological Constraints from Cluster Abundance and Weak Lensing *arXiv:2002.11124*
- Cluster cosmology with anisotropic boosts: Validation of a novel forward modeling analysis and application on SDSS redMaPPer clusters *arXiv:2112.09059*
- Dark Enrgy Survey Year 1 results: weak lensing mass calibration of redMaPPer galaxy clusters *arXiv:1805.00039*
- Optical selection bias and projection effects in stacked galaxy cluster weak lensing *arXiv:2203.05416*
- Dark Energy Survey Year 3 Results: Cosmological constraints from galaxy clustering and weak lensing *arXiv:2105.13549*

Thank you for your attention!